

# Structural and optical characterisation of double-doped TiO<sub>2</sub> nanoparticles

OO Nubi<sup>1</sup>, KE Rammutla and TE Mosuang

Department of Physics and Geology, University of Limpopo, South Africa

E-mail: olatunbosun.nubi@ul.ac.za

**Abstract.** With titanium isopropoxide as the precursor, single and double doped nanosized powders of TiO<sub>2</sub> were synthesised by the sol-gel process. The metal dopants used were Ag and Cu at doping levels of 5% (molar weight). The samples were dried at 100 °C in air and then heated at 300°C, 600°C, 900°C and 1100°C for one hour. Structural characterisation of the samples was carried out by X-ray Diffraction (XRD), Raman and Scanning Electron Microscopy (SEM) techniques. The results suggests that the co-doped TiO<sub>2</sub> powders are constituted by both the anatase and brookite phases whereas only anatase is observed in the case of pure and singly doped samples. The co-existence of brookite with anatase in the co-doped sample is thought to be responsible for the enhancement of anatase to rutile transformation. UV-visible measurements were done to study the optical properties of the TiO<sub>2</sub> nanoparticles. Double doping was found to enhance the narrowing of the band gap, compared to single doping.

## 1. Introduction

Titanium dioxide (TiO<sub>2</sub> or Titania) has been widely studied [1-4] because of its extensive applications in the fields of environment (photocatalysis, sensing) and energy (photovoltaics, hydrogen storage, water splitting, photochromics, electrochromics). It also finds uses as pigments [5], sunscreens [6], ointments [7], paints [8] and toothpaste [9]. Factors that determine the properties of the titania material used in these applications include phase composition, particle size and distribution, morphology as well as porosity [4].

In research and technological applications, the most important polymorphs of titania are the anatase (A), rutile (R) and brookite (B) crystalline phases [10]. Of these, rutile is the most stable while Brookite, being difficult to synthesize, is seldom studied [11]. The metastable anatase and brookite states begin to transform to rutile upon high temperature calcination between 600°C and 700°C. During synthesis, the formation of any particular phase is dependent on the precursors used, method of synthesis and the calcination temperature. It is of significant interest to understand the conditions that affect the transformation from one phase to another as this may affect the properties and performance of devices.

Recently, research studies have explored the effect of doping TiO<sub>2</sub>, via chemical synthesis, particularly with metal impurities [12]. Further, considerable enhancement of the photocatalytic activity and other characteristics has been observed for TiO<sub>2</sub> doped with two impurities as compared with single doping [13–16].

<sup>1</sup> To whom any correspondence should be addressed.

In this investigation, the effect of simultaneously introducing two metal dopants, via sol-gel synthesis, on the structural and optical properties of TiO<sub>2</sub> nanopowders, is compared with single-doped species. The Sol-gel method of synthesis affords a way of preparing nanosized materials by a chemical reaction in solution starting with metal alkoxide as a precursor. This route provides the advantages of attaining high chemical purity and precise control over pore structure and dopant concentration [4].

## 2. Experimental

### 2.1. Synthesis

In addition to the 'Undoped/TiO<sub>2</sub>' sample set, "single-doped" TiO<sub>2</sub> nanopowders (TiO<sub>2</sub> doped with either Cu and Ag), namely Ag/TiO<sub>2</sub>, Cu/TiO<sub>2</sub>, and one "double-doped" (TiO<sub>2</sub> doped with both Cu and Ag) set, Ag+Cu/TiO<sub>2</sub>, were synthesised at 5 wt% impurity level. Aldrich's analytical reagent grade precursors, namely Ti{OCH(CH<sub>3</sub>)<sub>2</sub>}<sub>4</sub> (Titanium (IV) Isopropoxide), AgNO<sub>3</sub> and CuCl<sub>2</sub>, were used to prepare the nanocrystalline TiO<sub>2</sub> samples via the sol-gel formulation. Priming, by first dissolving the dopant salts in water, was followed by adding ethanol to the required amount of each dissolved precursor. The dopant solution was then added, in drops, to the Titanium Isopropoxide, while vigorously stirring for up to 1 hour. The precipitate (xerogel) formed was further diluted with 30 ml water, filtered and left to dry at room temperature for 16 hours. Further drying of the samples was done at 100°C for 1 hour before being ground to powders.

The powdered samples were divided into four so that each could be annealed at temperatures of 300°C, 600°C, 900°C and 1100°C for one hour, thus making a total of 20 samples.

### 2.2. Characterisation

XRD powder data were recorded in the  $2\theta$  scan range of 10 – 90° with PANalytical X'Pert PRO diffractometer (Cu Ni-filtered K $\alpha$  radiation of  $\lambda = 1.540598 \text{ \AA}$ , operating at 45kV 40mA). Raman spectra from 50 to 1200 cm<sup>-1</sup> were obtained with a Jobin Yvon LabRAM HR 800 UV-VIS-NIR spectrometer equipped with an Olympus Microscope. SEM micrographs of the samples were obtained with a JEOL- JSM 7500F Scanning Electron Microscope. Optical absorption spectra were collected using Perkin Elmer Lamda 750S UV/Vis Spectrometer in the range of 200 – 800 nm, while the Perkin Elmer LS-55 Fluorescence Spectrometer was used for the Photoluminescence (PL) data.

The Scherrer equation,  $\tau_{(hkl)} = K\lambda/\beta_{(hkl)} \cos \theta$  was used in estimating the mean size  $\tau_{(hkl)}$  of the ordered crystalline domains from  $\beta_{(hkl)}$ , the line broadening at half the maximum intensity (or the full-width-at-half-maximum, FWHM) in radians. Here,  $\theta$  is the Bragg angle and  $\lambda$  is the X-ray wavelength (equal to 1.540598 Å for the Cu K $\alpha$  radiation used in this study). By considering the synthesised nanoparticles to be fairly spherically shaped, a value of 0.9 was assumed for the shape parameter (or roundness factor)  $K$  [17]. For quantitative comparative analyses, instrumental and strain broadening were neglected and Gaussian fitting of the most intense peaks of the individual phases – (101) and (200) for anatase and (110) and (211) for rutile – were carried out [14], with the aid of the Origin® statistical software package. The phase content of each sample was calculated from the integrated intensities of the respective peaks of anatase (101), rutile (110) and brookite (210) [12]

Many studies [18, 19] have employed direct-transition Tauc plot extrapolations in the investigation of the optical band gap for both thin films and nanostructured TiO<sub>2</sub>. This method requires a dimension-related parameter for estimating the absorption coefficients required in the determination of Kubelka-Munk function values. For instance, in the thin-films scenario, the parameter is often the thickness of the film. Determination of this parameter in the case of randomly sized nanoparticles is often not straightforward. Further, extrapolations of a Tauc plot can be somewhat ambiguous, particularly in cases where the linear region is not clearly defined. For these reasons, the Tauc route is not taken in this study. Instead, points on the absorption versus wavelength plot, which gives the sharpest change in absorption, are identified. This was achieved by plotting the absorption sensitivity to wavelength, (dA/d $\lambda$ ), against the wavelength (or photon energy) and selecting the position of the most intense peak. The peak thus obtained provide reasonable estimates of the energy gap between the conduction and valence bands for the samples under investigation.

### 3. Results and discussion

Nanocrystalline anatase  $\text{TiO}_2$  structure indexed to the American Mineralogist Crystal Structure Database (AMCSD) 0019093 were observed for the Undoped/ $\text{TiO}_2$ , as well as the single-doped  $\text{Ag}/\text{TiO}_2$  sample at calcination temperatures of  $600^\circ\text{C}$  and lower. At the higher temperatures of  $900^\circ\text{C}$  and  $1100^\circ\text{C}$ , these samples feature patterns that could be indexed to the AMCSD 000173 structure for rutile. This is in line with what is commonly found in literature for the anatase-to-rutile transformation at calcination temperatures above  $600^\circ\text{C}$ .

In figure 1 the XRD patterns are given for anatase (A) and rutile (R) samples calcined at  $600^\circ\text{C}$ . The presence of the well-formed rutile structure – for the  $\text{Cu}/\text{TiO}_2$  and the  $\text{Ag}+\text{Cu}/\text{TiO}_2$  powders at  $600^\circ\text{C}$  – suggests that the phase transition temperature (PTT) in these cases were lower than those of the Undoped/ $\text{TiO}_2$  and  $\text{Ag}/\text{TiO}_2$  samples. In particular, at  $300^\circ\text{C}$ , the double-doped  $\text{Ag}+\text{Cu}/\text{TiO}_2$  powder reveals peaks associated with the rutile phase, thus indicating the commencement of the phase change at this temperature. Although doping with Ag did not affect the transition in any appreciable way, the lowering of the transformation temperature by Cu was further enhanced by the inclusion of Ag impurities in the double-doped system.

This observation may be attributed to the presence of the brookite phase (figure 2) in the double-doped  $\text{Ag}+\text{Cu}/\text{TiO}_2$  sample between the calcination temperatures of  $300^\circ\text{C}$  and  $600^\circ\text{C}$ . With barely any anatase left untransformed at  $600^\circ\text{C}$ , the brookite phase content of the  $\text{Ag}+\text{Cu}/\text{TiO}_2$  sample was estimated to be 22.7%, the remaining 77.3% being rutile. The transformation of this brookite to rutile was found to be complete at  $900^\circ\text{C}$ .

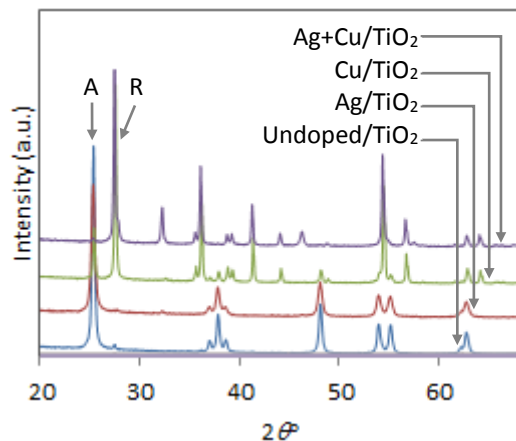


**Figure 1.** Anatase (A) and rutile (R) peaks in the XRD patterns of samples calcined at  $600^\circ\text{C}$ .

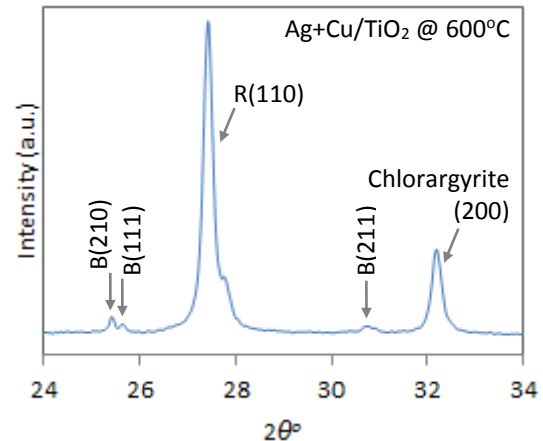


**Figure 2.** A zoom-in on the brookite (B) peaks present in the XRD patterns of the  $\text{Ag}+\text{Cu}/\text{TiO}_2$  sample calcined at  $600^\circ\text{C}$ .

The SEM micrographs of figure 3 belong to the Undoped/ $\text{TiO}_2$  at  $300^\circ\text{C}$  (left) and  $\text{Ag}/\text{TiO}_2$  at  $900^\circ\text{C}$  (right). Agglomeration of fairly spherically-shaped particulate structure, revealed in the images, are typical of what was observed for the anatase (at  $300^\circ\text{C}$ ) and the rutile (at  $900^\circ\text{C}$ ) phases.

Figure 4 displays how the crystallite size varies with increasing calcination temperature for the Undoped- $\text{TiO}_2$  samples. Judging by the 4<sup>th</sup>-order polynomial fit, the anatase sizes ( $100^\circ\text{C}$  to  $600^\circ\text{C}$ ) appear to grow relatively faster than the rutile ( $900^\circ\text{C}$  and  $1100^\circ\text{C}$ ). Further work, with smaller temperature intervals, may be needed to confirm this. However, the grains of doped powders are found to be smaller than those of the Undoped/ $\text{TiO}_2$ , (table 1), for the anatase structures, in agreement with other studies that discussed the reduction mechanism [20, 21].

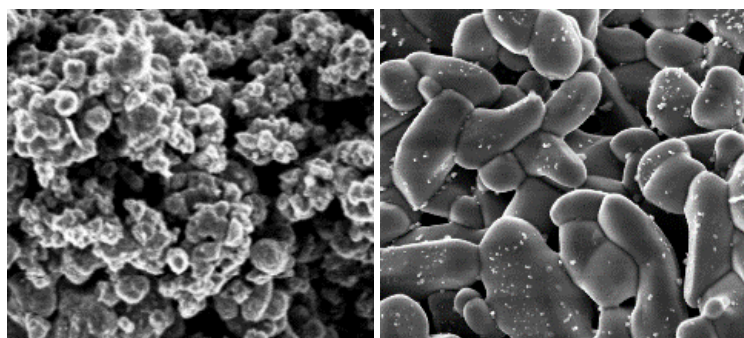


**Figure 3.** SEM micrographs of Undoped/TiO<sub>2</sub> at 300°C (left) and Ag/TiO<sub>2</sub> at 900°C (right).

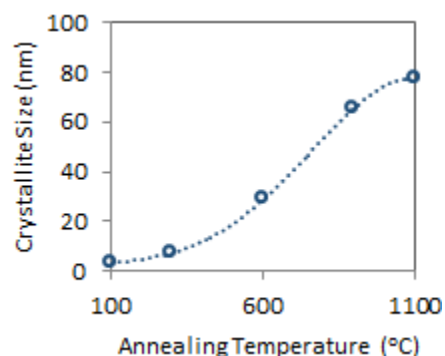


**Figure 4.** Crystallite size vs. calcination temperature of Undoped/TiO<sub>2</sub>.

**Table 1.** Crystallite sizes and lattice parameters for the anatase and rutile structures.

Sample	Anatase Structure at 300°C			Rutile Structure at 900°C		
	Crystallite size (nm)	Lattice Parameters (Å)		Crystallite size (nm)	Lattice Parameters (Å)	
		a = b	c		a = b	c
Undoped/TiO <sub>2</sub>	7.39	3.79	9.37	65.46	4.59	4.65
Ag/TiO <sub>2</sub>	6.17	3.80	9.09	74.93	4.59	2.96
Cu/TiO <sub>2</sub>	6.32	3.79	9.37	78.53	4.57	2.97
Ag+Cu/TiO <sub>2</sub>	4.65	3.79	9.21	79.69	4.58	2.96

The unit cell parameters (table 1) suggest that the TiO<sub>2</sub> lattice is not deformed by doping when in the anatase phase, whereas the rutile structure reduced in volume by about 36.4% with doping (even though the grain sizes became larger.)

In figure 5 the Raman scans are given for the Undoped/TiO<sub>2</sub> calcined at 300°C (Anatase) and at 900°C (Rutile). The spectrum for Anatase show the six characteristic bands usually identified at 144, 197, 399, 513, 519, and 639 cm<sup>-1</sup> with anatase TiO<sub>2</sub> [22, 23]. The Characteristic phonon modes of the rutile TiO<sub>2</sub> structures were also observed for all the samples constituted by the rutile phase. Here, the major peaks were found at 240, 446 and 610 cm<sup>-1</sup> while minor peaks are at 818, 707 and 319 cm<sup>-1</sup> as expected [24, 25]. The intensity and sharpness of the peaks signify that the samples are highly crystalline and pure. The results of the Raman spectroscopy thus compliment very well the results that were obtained from XRD. A blue-shift of about 6.3 cm<sup>-1</sup>, for both Cu/TiO<sub>2</sub> and Ag+Cu/TiO<sub>2</sub>, was evident in the Raman spectra of the anatase lowest-frequency mode (E<sub>g</sub>, due mainly to the symmetric stretching of the O–Ti–O). This blue-shift, displayed in figure 6 for all the powder sets calcined at 300°C, may be ascribed to phonon confinement, non-stoichiometry effects and variations in the dimensions of the nanoparticles [26, 27].

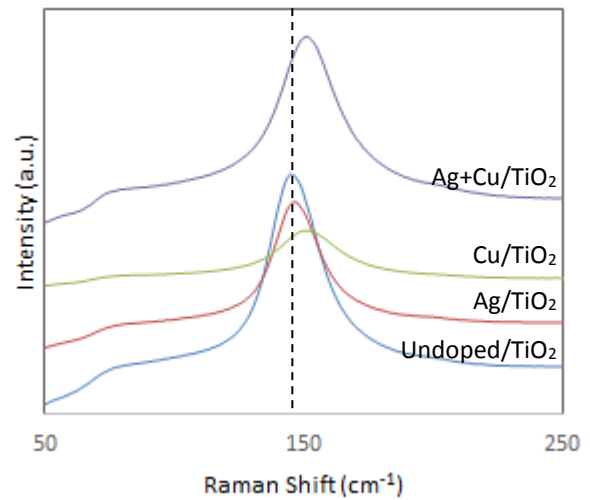
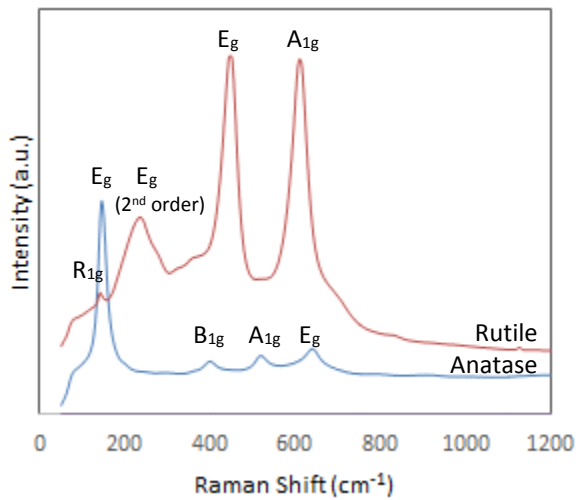


**Figure 5.** Raman spectra for the Undoped/TiO<sub>2</sub> calcined at 300°C (Anatase) and at 900°C (Rutile).

**Figure 6.** Raman spectra of the E<sub>g</sub> mode for samples at calcined at 300°C.

Figure 7 displays the optical absorption spectra of the sample sets at the various TiO<sub>2</sub> phases. Inset is the plot of the wavelength sensitivity of the absorbance versus the photon energy for the Undoped/TiO<sub>2</sub> calcined at 600°C. This yields a sharp peak (or the most rapid change in absorption) for this sample at 3.09 eV. Table 2 shows values for other samples that were derived in a similar manner. The band gap for the single-phase anatase powder Ag/TiO<sub>2</sub> was found to be 3.09 eV as well. The copper-doped (anatase-only) sample, Cu/TiO<sub>2</sub> however showed a red-shift towards a lower energy gap of 2.47 eV. This same improvement in photo absorptions was also observed for the Ag+Cu/TiO<sub>2</sub> sample which contains the mixed phase of anatase and brookite at 300°C. The narrowest band gap of 2.04 eV was observed for the brookite-rutile mix of Ag+Cu/TiO<sub>2</sub> at 600°C. In comparison, all the rutile-only samples (calcined at 900°C and above), doped and undoped, revealed a value of 3.08 eV.

Though others [28] have attributed it to quantum size effects, the shift of the absorbance spectra of Ag+Cu/TiO<sub>2</sub>, at 600°C, towards the visible light region may be ascribed to the introduction of some additional energy levels in the host lattice band gap by the impurities. As both Ag and Cu metals form a *p*-type semiconductor, a shift in Fermi energy towards valence band may be realised.

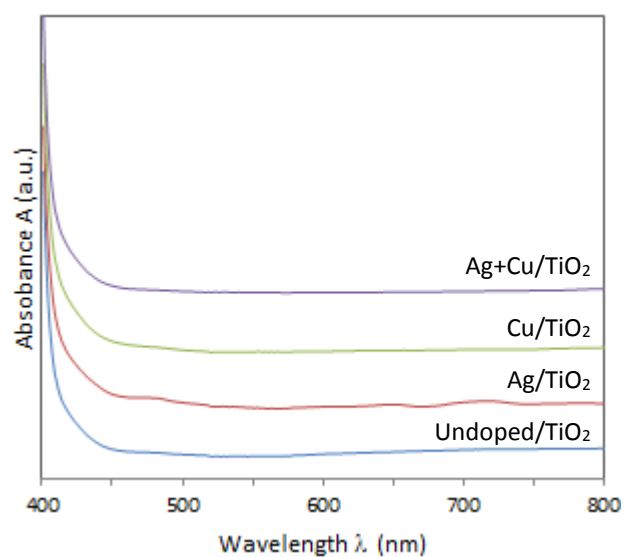
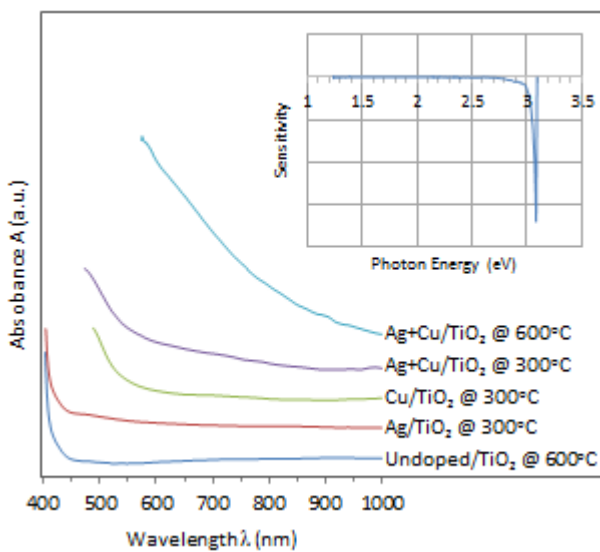


**Figure 7.** Optical absorption spectra of the sample sets at the various TiO<sub>2</sub> phases. Inset is the plot of the wavelength sensitivity of the absorbance versus the photon energy.

**Figure 8.** Optical absorption edges of the UV-vis spectra for the various sample sets at 900°C (rutile phase).

**Table 2.** Band gap of samples at various phase structures.

Sample	Calcination Temperature	Phases Present	Band Gap $E_g$ (eV)
Undoped/TiO <sub>2</sub>	600°C	Anatase	3.09
Ag/TiO <sub>2</sub>	300°C	Anatase	3.09
Cu/TiO <sub>2</sub>	300°C	Anatase	2.47
Ag+Cu/TiO <sub>2</sub>	300°C	Brookite, Anatase	2.47
Ag+Cu/TiO <sub>2</sub>	600°C	Brookite, Rutile	2.04
Ag+Cu/TiO <sub>2</sub>	1100°C	Rutile	3.08

#### 4. Conclusions

Double doping of TiO<sub>2</sub> with Ag and Cu impurities induced mixed phases which included brookite, namely, anatase-brookite (at 300°C) and rutile-brookite (at 600°C) before the transition to rutile TiO<sub>2</sub>. The presence of this brookite, though minute, appeared to lower the transition temperature appreciably. Even though doping reduced the grain size of TiO<sub>2</sub>, the anatase lattice was not deformed by doping but the rutile shrunk by 36.4%.

In general, single doping with silver did not alter the properties of TiO<sub>2</sub> as much as single doping with copper. For instance, due to phonon confinement, copper was able to introduce a blue-shift towards higher energies, in the Raman  $E_g$  mode. Optically, double doping featured a remarkable effect over the copper doped material by reducing the energy gap well into the visible region (608 nm, Yellow) of the electromagnetic spectrum. This could result in greater production of electron-hole pairs under visible light illumination and thus achieving higher photocatalytic efficiencies.

#### Acknowledgements

The authors would like to express their gratitude to NRF, IBSA and University of Limpopo for financial support and CSIR's Centre for Nanostructured Materials for experimental resources.

#### References

- [1] Mo S-D and Ching W Y 1995 *Phys. Rev. B* **51** 19
- [2] Hua C, Duoa S, Liua T, Xianga J and Li M 2010 *Appl. Surf. Sci.* **11**, 110
- [3] Colmenares J C, Aramedia M A, Marinas A, Marinas J M and Urbano F J 2006 *Appl. Catal. A-Gen.* **306** 120–7
- [4] Yu J-G, Yu J C, Cheng B, Hark S K and Iu K 2003 *J Solid State Chem.* **174**, 372–80
- [5] Pfaff G and Reynders P 1999 *Chem. Rev.* **99**, 1963
- [6] Salvador A, Pascual-Marti M C, Adell J R, Requeni A and March J G 2000 *J. Pharm. Biomed. Anal.* **22**, 22, 301
- [7] Zallen R and Moret M P 2006 *Solid State Commun.* **137**, 154
- [8] Braun J H, Baidins A and Marganski R E 1992 *Prog. Org. Coat.* **20**, 105
- [9] Yuan S A, Chen W H and Hu S S 2005 *Mater. Sci. Eng. C* **25**, 479
- [10] Murray C B, Norris D J and Bawendi M G 1993 *J. Am. Chem. Soc.* **115** 8706
- [11] Beltrán A, Gracia L and Andrés J 2006 *J. Phys. Chem. B* **110** 23417-23
- [12] Yang P, Lu C, Hua N and Du Y 2002 *Mater. Lett.* **57** 794–801
- [13] Chen D, Jiang Z, Geng J, Wang Q and Yang D 2007 *Ind. Eng. Chem. Res.* **46** 2741-46
- [14] Klug H P and Alexander L E, 1975 *J. Appl. Crystallogr* **8** 573-4
- [15] Yam M C, Chen F, Zhang J L and Anpo M 2005 *J. Phys. Chem. B* **109** 8673
- [16] Stengl V, Bakardjieva S and Bludska J 2011 *J. Mater. Sci.* **46** 3523

- [17] Langford J I and Wilson A J C 1978 *J. Appl. Cryst.* **11** 102-113
- [18] Hung W C, Chen Y C, Chu H and Tseng T K 2008 *Appl. Surf. Sci.* **255** 2205-13
- [19] Segne T A, Tirukkovalluri S R and Challapalli S, 2011 *Int. Res. J. Pure Appl. Chem.* **1** 3 84-103
- [20] Shin H, Jung H S, Hong K S and Lee J K 2005 *J. Solid State Chem.* **178** 15
- [21] Sheng Q R, Cong Y, Yua S, Zhang J L and Anpo M 2006 *Micropor. Mesopor. Mat.* **95** 220
- [22] Ohsaka T, Izumi F and Fujiki Y 1978 *J. Raman Spectrosc.* **7** 321
- [23] Porto S P S, Fleury P A and Damen T C 1967 *Phys. Rev.* **154** 522
- [24] Hardcastle F D and Ark J 2011 *Acad.Sci.* **65** 43
- [25] Katiyars R S, Dawsons P, Hargreaves M M and Wilkinson G R 1971 *J. Phys. C: Solid St. Phys.* **4** 2421–2431
- [26] Zhang W F, He Y L, Zhang M S, Yin Z and Cheng Q 2000 *J. Phys. D: Appl. Phys.* **33** 912–6
- [27] Mazza T, Barborini E, Piseri P, Milani P, Cattaneo D, Bassi A L, Bottani C E and Ducati C 2007 *Phys. Rev. B* **75** 045416
- [28] Chaudhary V, Srivastava A K and Kumar J 2011 *Mater. Res. Soc. Symp. Proc.* **1**.